Jinjin Ma
Department of Mechanical Engineering,
University of Michigan,
Ann Arbor, MI 48109

Kristen Goble
Department of Molecular and Integrative Physiology,
University of Michigan,
Ann Arbor, MI 48109

Michael Smietana
Department of Biomedical Engineering,
University of Michigan,
Ann Arbor, MI 48109

Tatiana Kostrominova
Department of Anatomy and Cell Biology,
Indiana University School of Medicine-Northwest,
Gary, IN 46409-1008

Lisa Larkin
Department of Biomedical Engineering,
and Department of Molecular and Integrative Physiology,
University of Michigan,
Ann Arbor, MI 48109

Ellen M. Arruda
Fellow ASME
Department of Mechanical Engineering,
University of Michigan,
Ann Arbor, MI 48109;
Macromolecular Science and Engineering Program,
University of Michigan,
Ann Arbor, MI 48109
e-mail: arruda@umich.edu

Morphological and Functional Characteristics of Three-Dimensional Engineered Bone-Ligament-Bone Constructs Following Implantation

The incidence of ligament injury has recently been estimated at 400,000/year. The preferred treatment is reconstruction using an allograft, but outcomes are limited by donor availability, biomechanical incompatibility, and immune rejection. The creation of an engineered ligament in vitro solely from patient bone marrow stromal cells (has the potential to greatly enhance outcomes in knee reconstructions. Our laboratory has developed a scaffoldless method to engineer three-dimensional (3D) ligament and bone constructs from rat bone marrow stem cells in vitro. Coculture of these two engineered constructs results in a 3D bone-ligament-bone (BLB) construct with viable entheses, which was successfully used for medial collateral ligament (MCL) replacement in a rat model. 1 month and 2 month implantations were applied to the engineered BLBs. Implantation of 3D BLBs in a MCL replacement application demonstrated that our in vitro engineered tissues grew and remodeled quickly in vivo to an advanced phenotype and partially restored function of the knee. The explanted 3D BLB ligament region stained positively for type I collagen and elastin and was well vascularized after 1 and 2 months in vivo. Tangent moduli of the ligament portion of the 3D BLB 1 month explants increased by a factor of 2.4 over in vitro controls, to a value equivalent to those observed in 14-day-old neonatal rat MCLs. The 3D BLB 1 month explants also exhibited a functionally graded response that closely matched native MCL inhomogeneity, indicating the constructs functionally adapted in vivo. [DOI: 10.1115/1.4000151]

1 Introduction

Ligament grafts are often required to replace tissue damaged by disease, surgery, or extensive trauma [1], in part, because the healing ability of ligament after any injury is relatively poor [2]. Limitations associated with grafting such as graft availability, donor site morbidity, and immune rejection have led investigators to develop strategies to engineer ligament tissue to reduce or eliminate the need for transplants altogether [2–8].

Current methodologies for engineering either ligament or bone utilize scaffolds that promote adhesion, migration, and proliferation of cultured fibroblastic or osteogenic cells. Both synthetic and biological materials have been investigated as potential scaffold materials for tissue-engineered knee ligament repair, including collagen, silk, biodegradable polymers, and composite materials, all with limited success [4,5]. While scaffolding strategies appear to promote fibroblastic or osteogenic cell growth, undesirable characteristics and failures such as low outcome measure scores, rupture, loss of stiffness and strength in vivo, immune rejection, improper scaffold degradation rates, and weak implant/native tissue interfaces have eliminated many tissue-engineered ligament approaches from further consideration in ligament replacement applications [8]. The mechanical property requirements of engineered ligament at the time of replacement remain under debate [4,5,8,9]. The current paradigm is to match or exceed native ligament stiffness and strength in order to restore stability to the knee [5]. Recent evidence suggests stiff scaffolds shield the cells within these structures from strains required for proper signal induction and hence growth of neoligamentous tissue [4,5,8]. The result is loss of viability with time in vivo and increased joint laxity [9,8]. Moreover, the stresses during normal anterior cruciate ligament (ACL) function do not typically exceed 20% of ACL strength [9], suggesting that current engineering approaches overdesign for strength, especially if eventual collagen growth and remodeling are expected with time. The compliance mismatch and dissimilar tissue interface between native bone and engineered ligament are other existing design issues that may impede clinical applications [2,10]. Therefore, an engineered ligament with engineered bone at each end—reminiscent of the bone-ligament-bone patellar tendon graft—that can integrate into the recipient bone and form a mechanically viable and biochemically relevant interface between the two tissues would be optimal for replacement.

To address the need for structurally and biochemically relevant engineered ligaments and bone/ligament interfaces, and to avoid limitations associated with scaffold-based approaches, scaffold-

Contributed by the Bioengineering Division of ASME for publication in the JOURNAL OF BIOMECHANICAL ENGINEERING. Manuscript received November 15, 2008; final manuscript received August 4, 2009; accepted manuscript posted September 3, 2009; published online xxxxx-xxxxx-xxxxx. Editor: Michael Sacks.

less approaches to tissue engineering have begun to emerge. Hairfield-Stein et al. [11] used porcine bone marrow stromal cells (BMSCs) to generate self-organized rodlike tissues with silk suture segments as anchor points in a 14 day culturing period. Our laboratory has previously developed a scaffoldless method to engineer three-dimensional (3D) ligament construct (ELC) and bone construct (EBC) from rat bone marrow stromal cells (BMSCs) in vitro [12,13], as well as a method to coculture the ELCs and EBCs to engineer an in vitro 3D tissue model called a bone-ligament-bone (BLB) construct [12].

The purpose of the present study was to investigate the potential viability of utilizing 3D constructs engineered from a patient's own BMSCs for tissue replacement during knee ligament reconstruction. We hypothesized that these constructs have the ability to withstand hyperphysiological strain levels in vivo, will exhibit physical growth and collagen content increases with time in vivo, and will form viable interfaces with native bone tissue with time in vivo. Due to the small size and limited accessibility of the rat ACL, we fabricated BLBs from rat BMSCs, utilized these constructs for MCL (a more accessible knee ligament) replacement and compared their morphology and mechanical properties to those of 3D BLBs fabricated, and cultured 4 weeks in vitro and of native MCL. Following 1 and/or 2 month recovery, the 3D BLB constructs were analyzed for incorporation into native bone, functional, structural, size, and histochemical advances in the bone and ligament sections of the implant, and recovery of knee mechanics in the recipient.

2 Methods

2.1 Animal Model and Animal Care. Female Fischer 344 rats obtained from the Charles River Laboratories, Inc. (Wilmington, MA) were used. All animals were acclimated to our colony conditions, i.e., light cycle and temperature, for 1 week prior to any procedure. Rats were housed in hanging plastic cages (28 $\times$56 cm^2) and maintained on a 12 h/12 h light/dark cycle at a temperature of 20–22°C. The animals were fed Purina Rodent Chow 5001 laboratory chow and were given free access to water. All surgical procedures were performed in an aseptic environment with animals in a deep plane of anesthesia induced by intraperitoneal (i.p.) injections of sodium pentobarbital (50 mg/kg). Supplemental doses of pentobarbital were administered as required to maintain an adequate depth of anesthesia. Following any surgical procedure, the animals were singly housed until the date of explantation. All animal care and animal surgeries were in accordance with The Guide for Care and Use of Laboratory Animals (Public Health Service, 1996, NIH Publication No. 85-23); the experimental protocol was approved by the University Committee for the Use and Care of Animals.

2.2 Preparation of Solutions and Media. Unless otherwise indicated, all solutions and media were prepared and stored at 4°C prior to the isolation and culture of cells and warmed to 37°C in a heated water bath immediately prior to use. The media, with slight modifications from Refs. [14,15], were as follows: for ligament, growth medium (GM) consisted of 400 ml of Dulbecco's modified eagle medium (DMEM) (Gibco, Rockville, MD, Cat. No. 10565-042) with 100 ml fetal bovine serum (FBS) (Gibco, Rockville, MD, Cat. No. 10437-028), 6 μg/ml fibroblast growth factor basic (FGFb) (Peprotech, Rocky Hill, NJ, Cat. No. 100-18B), 0.13 mg/ml asc-2-phos (Sigma, St. Louis, MO, Cat. No. A8960-5G), 0.05 mg/ml L-proline (Sigma, St. Louis, MO, Cat. No. P5607-25G), and 5 ml antibiotic-antimycotic (Sigma, St. Louis, MO, Cat. No. A9909), and differentiation medium (DM) consisted of 460 ml DMEM with 35 ml 100% horse serum albumin (HSA) (Gibco, Rockville, MD, Cat. No. 16050-122), 0.13 mg/ml asc-2-phos, 0.05 mg/ml L-proline, 2 ng/ml transforming growth factor-beta (TGF-β) (Peprotech, Rocky Hill, NJ, Cat. No. 100-21), and 5 ml antibiotic-antimycotic (Sigma, St. Louis, MO, Cat. No. A9909). For bone, the growth and differentiation media were the same as GM and DM, respectively, with the addition of $10^{-8}M$ dexamethasone (DEX) (Sigma, St. Louis, MO, Cat. No.D4902-25MG).

2.3 Preparation of Culture Dishes. BLB constructs were engineered in individual 35 mm plates. Briefly, each 35 mm plate was coated with 1.5 ml of Sylgard (Dow Chemical Corporation, Midland, MI, type 184 silicon elastomer) and allowed to cure for 3 weeks prior to use. Sylgard coated plates were then coated with laminin at 3.0 $\mu g/cm^2$ per plate (30 μg of natural mouse laminin (Gibco, Rockville, MD, Cat. No. 23017-015) and 3 ml of Dulbecco's phosphate-buffered saline (DPBS) *p*H 7.2 (Gibco, Rockville, MD, Cat. No. 14190-144 per plate) and dried for 48 h. Salt crystals were dissolved and removed by rinsing the plates with 3 ml DPBS. The plates were then filled with 2 ml of previously described GM, decontaminated with UV light (wavelength of 253.7 nm) for 90 min, and placed in a 37°C, 5% CO_2 incubator for 1 week prior to plating BMSC.

2.4 Bone Marrow Stem Cell Isolation and Expansion. Surgical procedures were performed to remove both femurs for the isolation of BMSCs. The marrow was flushed from the donor bone tissue using a syringe with an $18\frac{1}{2}$-gauge needle filled with GM. The marrow was further dissociated by mixing with a $21\frac{1}{2}$-gauge needle before being centrifuged at 480 g for 5 min at 25°C. The pellet was resuspended in 10 ml GM (as appropriate for constructs under construction, ligament versus bone) and plated into 100 mm diameter tissue culture dishes. The dishes were kept in an incubator at 37°C, 95% humidity, and 5% CO_2. After 48 h, the nonadherent cells were removed by rinsing with DPBS. The adherent BMSC were cultured to 80% confluence, at which time the cells were enzymatically removed from the 100 mm plates using a 0.25% trypsin-EDTA solution (Gibco, Rockville, MD, Cat. No. 25200-072) and passaged. Cells were plated onto prepared culture dishes within the third and fifth passages.

2.5 Preparation of Self-Organized Bone Constructs. After pre-incubation, the GM was aspirated and 2×10^5 cells per 35 mm dish were seeded onto each laminin-coated Sylgard plate, after which the bone GM was changed at 2–3 days. After approximately 3 days, when the cells became confluent, bone DM was substituted to induce construct formation. The DM was changed every 2–3 days until the constructs were ready to coculture with ligament.

2.6 Bone-Ligament-Bone Construct Formation. The GM was aspirated from additional laminin-coated Sylgard plates and 2 ml of the ligament cell suspension containing 2×10^5 cells/ml GM were plated in each 35 mm culture dish. The plates were maintained in a 37°C, 5% CO_2 incubator and the ligament GM was changed at 2–3 days. After the cells became confluent, approximately 3 days later, engineered bones (fabricated as described above) were cut into two segments and each segment was pinned using two minutien pins on top of the ligament cell monolayer such that the proximal bone construct ends were 10 mm apart. Following bone pinning, GM was replaced with ligament DM and this ligament DM was changed every 2–3 days. Approximately 1 week following the introduction of DM, the ligament monolayer rolled up around the bone construct forming a 3D BLB construct with a total length of 15 mm (Fig. 1(*a*)). All constructs were held in culture and fed fresh DM every 2–3 days for 1 week, at which point six constructs were used for medial collateral ligament (MCL) 1 month replacement and three constructs were used for 2 month replacement. The remaining constructs were held in culture an additional 4 weeks to serve as time matched controls for the in vivo studies. Of these six 1 month explanted constructs, two were prepared for histological analysis and four for cyclic tension tests. All three 2 month explanted constructs were prepared for histological analysis.

2.7 MCL Replacement Via Engineered BLB Constructs.

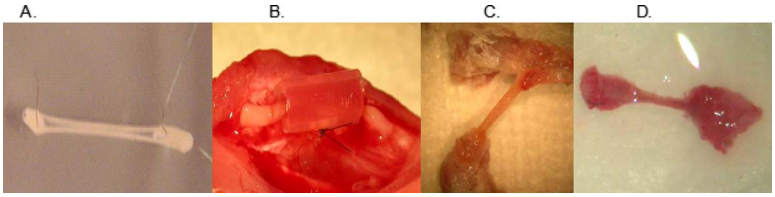

Fig. 1 Fabrication, implantation, and explantation of 3D BLB constructs engineered in vitro for medial collateral ligament replacement. (*a*) BLB construct just prior to implantation; approximately 3 days after detachment of the monolayer, the cells self-organized into a cylinder. Total length of the construct pin to pin=15 mm; diameter=0.47 mm. (*b*) 3D BLB from image (*a*) placed inside silicone tubing and secured in replacement of excised MCL. (*c*) 3D BLB construct 4 weeks following implantation. The presence of the silicone tubing makes it easy to visualize and excise the implanted construct; following 1 month of implantation, the engineered BLB has fused with the bone at the femur and tibia and increased in diameter to 0.53 mm. (*d*) 3D BLB excised from bone to be used for histology.

Six BLB constructs fabricated from the isolated BMSCs were used as MCL replacements in host rats (Figs. 1(*b*)–1(*d*)). The rat MCL replacement model was used because the size of the adult native rat MCL (12×3 mm^2) is approximately the same as that of our engineered BLB construct (15×0.47 mm^2). Additionally, the MCL is superficial, providing easy access to bone at the femur and the tibia, thus simplifying both the replacement of ligament and the recovery from the surgical procedures. Briefly, the distal medial head of the femur and proximal medial head of the tibia were exposed. The muscle and connective tissue surrounding the MCL were reflected exposing the MCL, which was severed from its points of insertions on both the femur and tibia. The native MCL was preserved for subsequent analysis of structure and function. A Dremel drill was used to drill 0.9 mm holes at the points of MCL insertion on the femur and tibia. A portion of the ligament region of the engineered BLB construct was surrounded by a 1.6 mm inner diameter (ID) diameter silicone tube for subsequent identification during explantation (Fig. 1(*b*)), and the bone sections of the construct were inserted into the drill holes. The constructs were secured to the bone by suturing them to the surrounding connective tissue. Finally, the muscle layers were closed using 7-0 suture and the skin was closed using 4-0 suture. Within 1 h, animals were awake and resumed normal cage activities of eating and drinking. All animals were allowed to recover for either 1 or 2 months before the removal of the BLB explants. Prior to surgery and following the recovery period and prior to construct explantation, all animals were assessed for locomotor function using foot print analysis and rotorod testing [16]. Either 1 or 2 months following the explantation, the entire knee was extracted from the animal (Fig. 1(*c*)), the engineered construct was isolated from surrounding tissues, and the patellar tendon, ACL, posterior cruciate ligament, and lateral collateral ligament were excised leaving the BLB-based MCL replacement tissue adhered to the femur and tibia (Fig. 1(*d*)). The explanted BLB constructs were either fixed for histochemical analysis or briefly placed in transfer media (DPBS with 2% antibiotics) prior to mechanical testing.

2.8 Native MCL Dissections. Pregnant Fischer 344 rats were obtained at 13 days into the gestation and acclimated under the same conditions as previously described. 14 days following the birth of the pup rats were euthanized with an overdose of sodium pentobarbital (100 mg/kg) administered by intraperitoneal injection. The legs were dissected, removing the skin and muscle but maintaining the ligament connections at the knee. The MCL ($n=5$) was isolated by removing all other knee ligaments. The tibia and femur were cut midbone to provide tissue for gripping during mechanical testing. Both MCLs were removed from the rat and fixed for histochemical analysis.

2.9 Histochemical and Immunohistochemical Analysis of 3D BLB Constructs and Native MCLs. For histochemical staining, unfixed samples were placed into TBS medium, frozen in cold isopentane and stored at −80°C until needed. Three to five samples per group of 3D BLB constructs developed in vitro and after implantation in vivo were analyzed. Samples were sliced longitudinally with a cryostat at a thickness of approximately 12 μm, adhered to Superfrost Plus microscopy slides, and used for staining. Sections were stained for general morphology observations with hematoxylin and eosin (H&E). Immunofluorescent staining with specific antibodies was performed to detect the presence of blood vessels (CD-31), collagen type 1, and elastin. Frozen sections were fixed with ice cold methanol for 10 min and rinsed three times with phosphate-buffered saline (PBS). Sections were blocked for 30 min with PBS-0.05%Tween20 (PBST) containing 20% calf serum (PBST-S) at room temperature. Sections were incubated overnight at 4°C with the primary antibodies in PBST-S. The concentrations of each of the primary antibodies were as follows: 10 μg/ml of rabbit antirat collagen type 1 (Abcam, Cambridge, MA), 10 μg/ml of rabbit antirat elastin (Chemicon, (Millipore), Billerica, MA) and 20 μg/ml of mouse antirat CD31 (AbD Serotec, Oxford, UK). 1 h room temperature incubation with Cy3-conjugated antimouse or antirabbit antibody (Jackson ImmunoResearch Laboratory, West Grove, PA) was used for visualization. Costaining of sections with fluorescein labeled wheat germ agglutinin (WGA) 5 μg/ml, Molecular Probes, Eugene, OR) was used for general visualization of the sample structure. Nuclei were stained by 5 min incubation with a DAPI solution (Sigma, St. Louis, MO) in PBST. The sections were examined and photographed with a Leica microscope.

2.10 Mechanical Evaluation of BLBs and Native MCLs. Cyclic tensile tests on BLB constructs and native MCLs were conducted to obtain poroviscoelastic responses to multiple load/unload cycles, calculate tangent stiffness during the initial load excursion, examine the mechanical heterogeneity of the ligament response, and evaluate the mechanical integrity of the engineered enthesis. An in-house designed tensiometer was employed to conduct the cyclic tension. A chamber located in the middle of the tensiometer has two grips protruding into the chamber that are connected to stepper motors. The chamber is filled with saline to test the specimens in hydrated conditions. The bones at the ends of the specimens were secured into the grips by clamping pressure, whereas the ligament and enthesis regions were well away from the grips to eliminate stress or strain concentrations on these tissues. The specimen diameter was measured at several positions along the length using an inverted microscope (Axiovert 25 at $\times50$ magnification, Carl Zeiss, Thornwood, NY), allowing the

average diameter of the ligament portion to be calculated. Blue microsphere fiduciary markers (25 μm diameter, 403-025 IMT, Irvine, CA) were brushed on the surface of the ligament portion of the constructs for digital image correlation analysis of tissue displacements to provide highly accurate calculations of the tissue strain field along the entire ligament. Images of the deforming tissues were taken using a 1.4 megapixel digital video camera (Basler, Ahrensburg, Germany) mounted on the microscope. 3D BLB and native MCL samples were loaded in the tensiometer under cyclic tension loading (0–10% strain, 0.01 Hz), and the synchronized force and image recordings were compiled and controlled by LABVIEW software (National Instruments, Austin, TX) on a Dell Precision 300 computer. Five load-unload cycles were conducted to characterize the overall nonlinear poroviscoelastic response based on the average strain along the section length of the ligament portion of the BLBs and native MCLs. These same cyclic loading data were used with the local strain field measurements to examine the functionally graded response of the engineered or native ligament. A maximum strain of 10% was chosen to examine the cyclic response within the MCL.

Force versus digital image data were converted to nominal stress versus nominal strain, where the nominal stress σ and strain ε are defined as follows:

$$\sigma = \frac{F}{A}, \quad \varepsilon \frac{l_c - l_o}{l_o}$$

where F is the force, and A is the cross-sectional area measured before testing. l_c and l_o stand for the current length and original length, respectively. The stress was computed by normalizing the load data by the average cross-sectional area of the samples. Strain data were analyzed using the image processing functions in the imaging software package METAMORPH, a 2D DIGITAL IMAGE CORRELATION method, and a preprocessing data smoothing technique in MATLAB (MathWorks, Inc. Natick, MA). The images generated during the tests were loaded as a stack into METAMORPH, and the object tracking function generated displacement value sheets of targeted markers. Nominal strains between markers were calculated and smoothed with a Savitzky–Golay filtering method to reduce any vibration effects (MathWorks, Inc. Natick, MA). Smoothed strain data were combined with the synchronized nominal stress data to create the cyclic nominal stress versus nominal strain response curves for each specimen. The (maximum) tangent stiffness was determined by calculating the maximum value of the slope of the nominal stress versus the nominal strain response of the initial load cycle. Displacement continuity was verified across the engineered enthesis of BLB samples to verify structural integrity over the cyclic strain range.

3 Results

3.1 Morphology of 3D BLB Constructs In Vitro. Prior to utilization for implantation, histological analysis of the BLB constructs with H&E showed the presence of areas resembling bone at both ends of the constructs (Fig. 2(*a*)). Fibrous middle part of the BLB constructs resembled ligament (Fig. 2(*a*)). At the higher magnification, collagen 1 stained bone portion showed dense deposits of collagen (Figs. 2(*b*) and 2(*d*)) similar to those found in the developing bone in vivo. Collagen 1 immunostaining of the ligament portion of the BLB construct revealed well aligned longitudinally oriented collagen fibers, some evidence of crimp morphology and elongated nuclei between fibers (Figs. 2(*c*) and 2(*e*)). The middle part of the BLB constructs also stained positive for elastin (Fig. 2(*f*)).

3.2 Morphology of 3D BLB Explants After Performance as Rat MCL Replacement Tissue. During either 1 or 2 months of implantation, the BLB constructs replaced the MCL in the left leg of the host rat model. Both 1 and 2 month explants were comparable in structure with 2 month explants showing slightly more advanced structural features; therefore, only the 2 month explants data are shown. Detailed analysis of the 2 month explants is discussed below. When explanted, the constructs were integrated well into the native bone at both the tibial and femoral sites (Fig. 3) and were supplied by the blood vessels generated from the host animal. Longitudinal sections of the middle of BLB explants were stained with H&E (Fig. 4). Collagen fibers filled the entire middle part of the explant with more cellular areas located at the periphery (Figs. 4(*a*)–4(*c*)). While the collagen fibers in the explants were highly organized and resembled that of native adult rat MCL (Fig. 4(*e*)), the explants displayed a higher nuclei per collagen fiber ratio placing them between neonatal (Fig. 4(*d*)) and

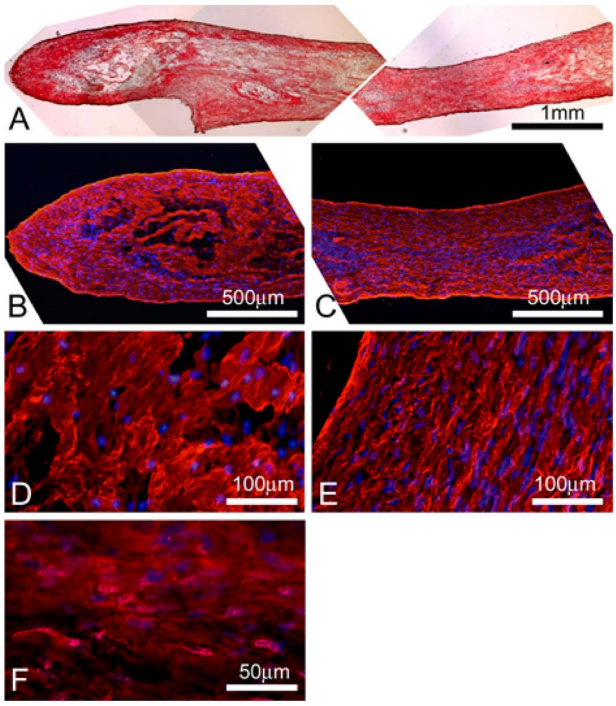

Fig. 2 Histological evaluation of the of 3D BLB construct developed in vitro. (*a*) H&E staining. ((*b*) and (*d*)) Collagen 1 immunostaining (red) of the end of the construct. ((*c*) and (*e*)) Collagen 1 (red) immunostaining of the middle part of the construct. (*f*) Elastin immunostaining (red) of the middle part of the construct. DAPI staining (blue) was used to visualize the nuclei.

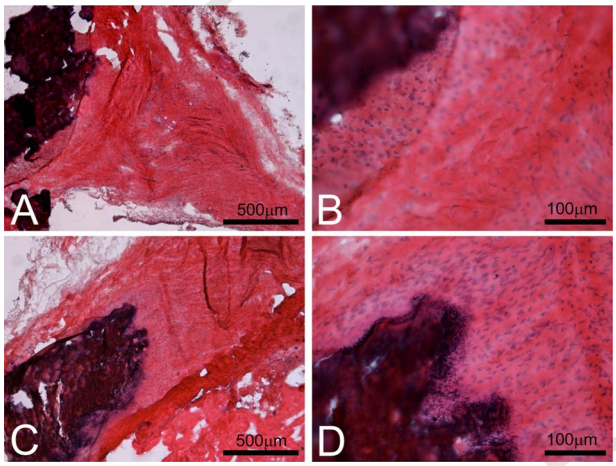

Fig. 3 H&E staining of areas of native bone/3D BLB construct interfaces at the tibia ((*a*) and (*b*)) and femur ((*c*) and (*d*)) sides after 2 months of implantation

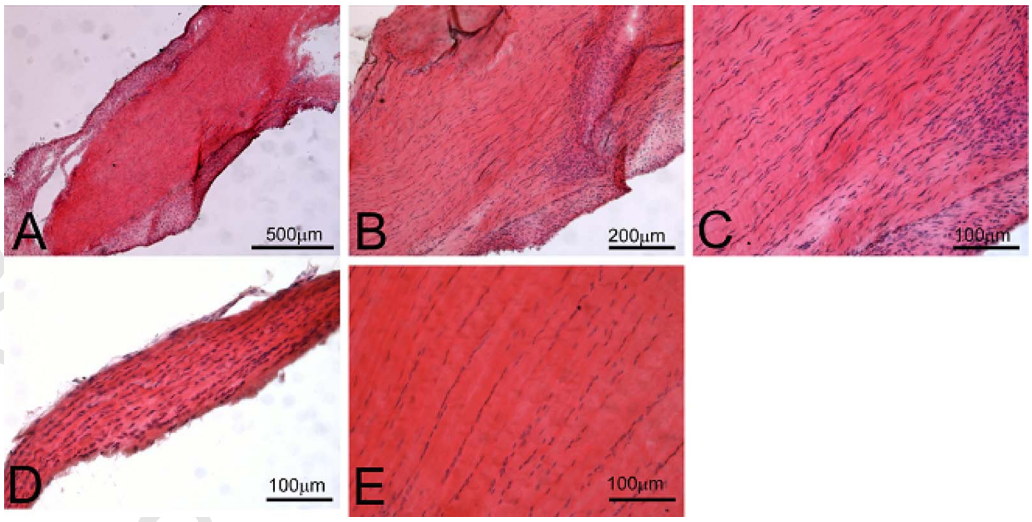

Fig. 4 H&E staining of the middle part of the 3D BLB construct after 2 months of implantation ((*a*)–(*c*)) and native MCL ligament from 21 day old neonatal (*d*) and from adult (*e*) rat

adult (Fig. 4(*e*)) MCL. Immunostaining of the middle of the BLB explants for collagen 1 (Figs. 5(*a*) and 5(*b*)) showed patterns of more densely packed collagen fibers than those found in neonatal MCL (Fig. 5(*c*)) and more closely resembled collagen 1 staining of adult rat MCL (Fig. 5(*d*)). Blood vessels were easily detected at the periphery of the middle part of the BLB explants (Figs. 6(*a*) and 6(*b*)). The degree of vascularization was slightly higher than that found in the native neonatal (Fig. 6(*c*)) and adult (Fig. 6(*d*)) rat MCL. The elastin immunostaining of the middle of the BLB explants detected very thin longitudinally oriented elastic fibers (Fig. 7(*a*)). The elastin content was higher than that found in the 3D BLB constructs in vitro but lower than in the native neonatal (Fig. 7(*c*)) and adult (Fig. 7(*e*)) rat MCL.

3.3 Cyclic Mechanical Tension Tests on BLB Constructs and Native MCL. Five sequential load-unload tension response curves are shown for in vitro 3D BLB constructs (Fig. 8(*a*)), 3D BLB 1 month explants (Fig. 8(*b*)), and native 14 day neonatal rat MCL (Fig. 8(*c*)). The in vitro constructs displayed the characteristic nonlinear soft tissue response that included an initial toe region followed by strain hardening. The ligament tangent stiffness of these constructs was 14.3 ± 3.0 MPa ($n=4$, Fig. 9). They also displayed hysteresis in the initial load-unload response, characteristic of poroelastic and viscoelastic materials, and the subsequent cycles overlapped the first. After 1 month of implantation, the ligament explants grew physically in size and their tangent stiffness increased on average by a factor of 2.4 to 34.6 ± 17.1 MPa ($n=4$, Fig. 9). The BLB explants had a cross-sectional area of 0.25 ± 0.17 mm^2, which is approximately twofold greater than that of 14 day neonatal rat MCL (0.12 ± 0.06 mm^2). The toe region in the mechanical response of the BLB explants transitioned to strain hardening more gradually and at lower strain levels than those of in vitro controls, and strain softening behavior was observed in some specimens. The BLB constructs in vitro and upon explantation all demonstrated mechanically viable entheses that withstood the cyclic strain protocol without separation or tearing of the interface. The native 14 day neonatal MCL exhibited a similar cyclic loading response (Fig. 8(*c*)) to that of the 3D BLB explants (Fig. 8(*b*)) including a similar transition from the toe region to strain hardening and approximately the same tangent stiffness as the BLB explants, 47.6 ± 22.9 MPa ($n=5$, Fig. 9).

The peak load experienced by the BLB explant in Fig. 8(*b*) during cyclic tension testing was $P_{max}=0.7$ N, measured at a peak strain of $\varepsilon=0.083$. The native MCL in Fig. 5(*c*) experienced $P_{max}=0.25$ N during a similar test protocol and measured at $\varepsilon=0.095$. The cross-sectional area of a BLB explant and hence its geometric stiffness (P_{max}/peak strain) exceed that of the native MCL by a factor of approximately 2.0; therefore, the BLB explant carried a higher load than the native MCL at a similar strain level.

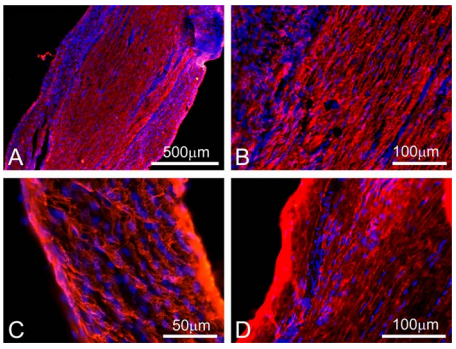

Fig. 5 Immunostaining of the middle part of 3D BLB construct after 2 months of implantation ((*a*) and (*b*)) and native MCL ligament from 21 day old neonatal (*c*) and from adult (*d*) rat with antibodies against collagen 1 (red). DAPI staining (blue) was used to visualize the nuclei.

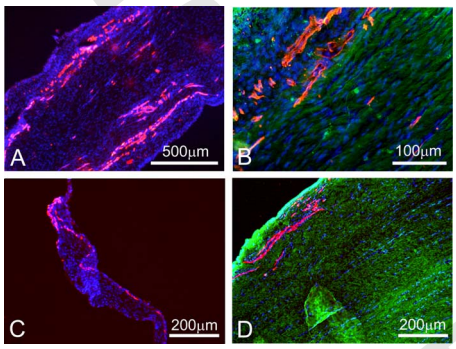

Fig. 6 Immunostaining of the middle part of 3D BLB construct after 2 months of implantation ((*a*) and (*b*)) and native MCL ligament from 7 day old neonatal (*c*) and from adult (*d*) rat with antibodies against CD31 (red) to visualize blood vessels. DAPI staining (blue) was used to visualize the nuclei. WGA lectin-fluorescein (green) was used to visualize the general tissue structure.

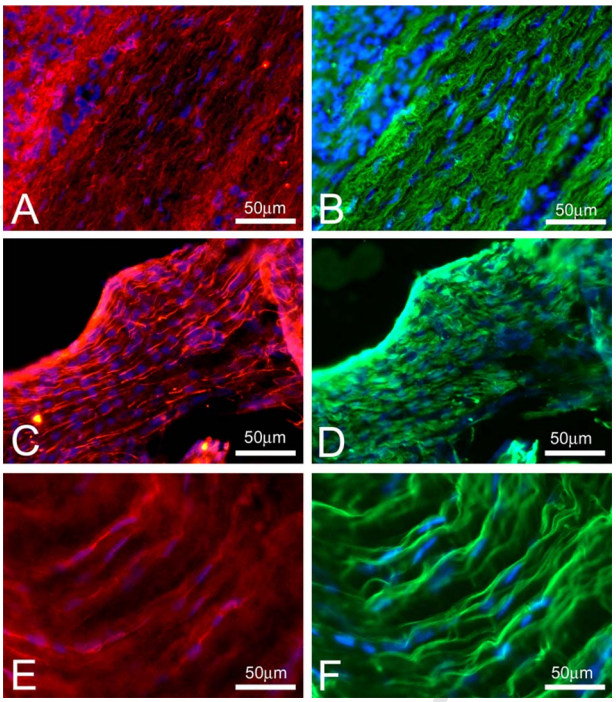

Fig. 7 Immunostaining of the middle part of 3D BLB construct after 2 months of implantation (*a*) and native MCL ligament from 7 day old neonatal (*c*) and adult (*e*) rat with antibodies against elastin (red). DAPI staining (blue) was used to visualize the nuclei. WGA lectin-fluorescein ((green in (*b*), (*d*), and (*f*)) was used to visualize the general tissue structure in 3D BLB construct (*b*), 7 day old neonatal (*d*), and adult (*f*) rat.

Representative local mechanical response curves are shown for in vitro 3D BLB constructs (Fig. 10(*a*)), 3D BLB 1 month explants (Fig. 10(*b*)), and native adult rat MCL (Fig. 10(*c*)). Regions were chosen from 2 mm to 4 mm long sections near the bone insertions and from the midsection along the ligament portion. Local stress versus strain response curves from both ends and the midsection of the in vitro constructs lie on top of each other, indicating a homogeneous mechanical response. However, after 1 month of implantation, the 3D BLB constructs developed an inhomogeneous strain response along their length. The midsection of the ligament portion is relatively stiff (curves shown in blue) compared with the ends of the ligament where it inserted to the bones (curves shown in red), showing a functionally graded strain response in vivo. The native adult rat MCL exhibited a similar functionally graded pattern to that of the BLB explants; the ends of ligament are more compliant and the middle section is stiffer.

3.4 Footprint Analysis. Analysis of gait and foot placement via methods of foot print analysis showed no significant differences between the walking pattern of the animal before and after surgery, indicating full recovery of knee function using BLB constructs for replacement after 4 weeks (data not shown).

4 Discussion

Given the proper environment, BMSCs can differentiate into many types of mesenchymal lineages including bone, ligament, tendon, cartilage, muscle, nerve, and fat [17,6]. BMSCs have demonstrated advantages over differentiated cells such as ACL fibroblasts that may render them optimal for ligament engineering, and their potential for tissue regeneration is the subject of ongoing investigations. BMSCs have more freedom of differentiation and self-renewal, while the differentiation of fibroblasts from ligament and tendon tends to be monotonic. Moreover, the proliferation system of BMSCs is robust and their adaptability to local envi-

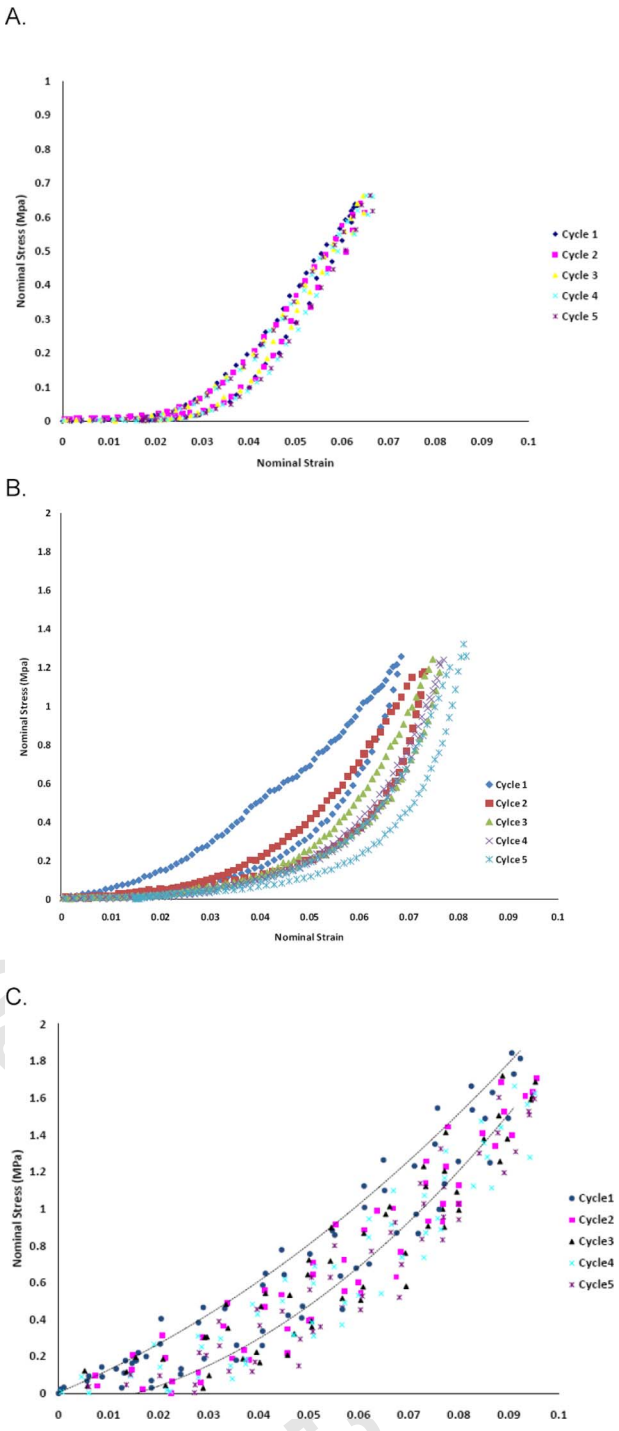

Fig. 8 Nominal stress versus nominal strain cyclic response curves for in vitro 3D BLBs, 3D BLB explants, and 14 day native MCLs. (*a*) Stress-strain response of the in vitro 3D BLBs shows that the nonlinear cyclic response includes a toe region, strain hardening, and hysteresis. (*b*) Stress-strain response of 3D BLB explants after 4 weeks as MCL replacement tissues on a stress scale that is (approximately) twice that in (*a*), indicating an increase in mechanical stiffness of the construct during in vivo implantation. The nonlinear response includes hysteresis and an earlier and more gradual transition to strain hardening than in the in vitro BLBs. (*c*) Stress-strain response of native 14 day neonatal MCL shows similar nonlinear stress-strain cyclic behavior to that observed in the 3D BLB explants.

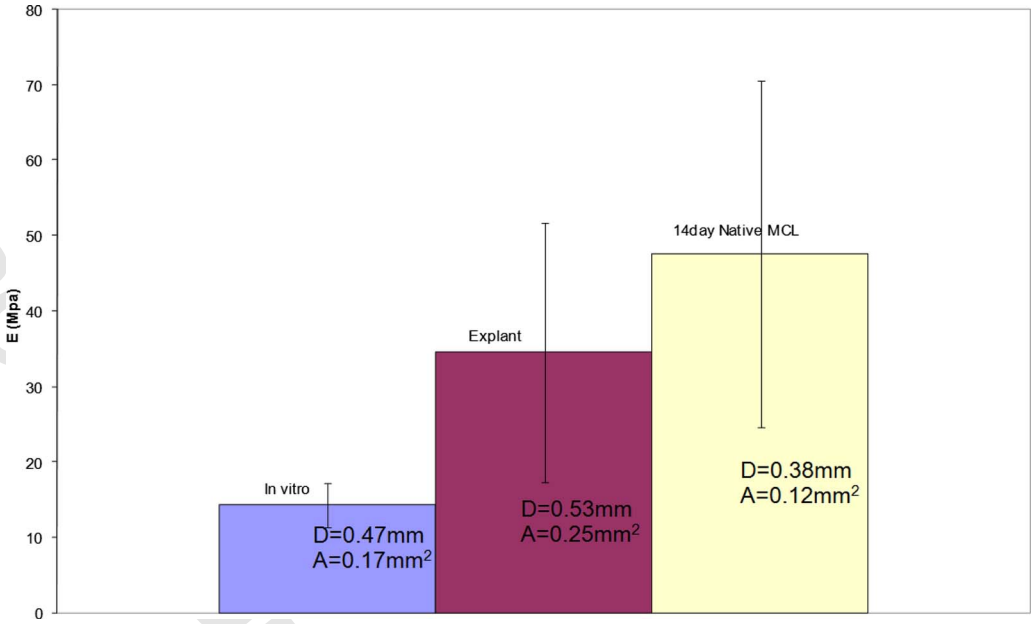

Fig. 9 Comparison of tangent stiffness, average diameter, and cross-sectional area of in vitro 3D BLBs, 3D BLB explants, and 14 day native MCLs

ronments (in vitro investigation) is strong [4,7]. Previous studies have shown the requirements for driving BMSCs to bone in vitro are ascorbic acid, DEX, TGF-β, FGFb, and an organic phosphate [18–24]. In contrast, BMSCs cultured in TGF-β, FGFb, and ascorbic acid in the absence of DEX can be driven to a ligament lineage [12,25,26]. Using these specific growth factors on BMSCs during proliferation and differentiation in vitro, we have successfully fabricated ELCs and EBCs [12,13]. Furthermore, coculturing these two types of constructs enabled us to generate 3D BLB constructs with viable entheses [12].

Since a single specific marker does not exist for either bone or ligament, characterization of these BMSC-derived tissue types involves morphological observations of cellular and ECM structures and the presence of the expected cell biomarkers generally found in neonatal bone and ligament. For bone, the presence of alkaline phosphatase, an enzyme that cleaves phosphate ions from organic molecules, is a precursor to mineralization and thus an early sign of bone formation [27]. Type 1 collagen mineralized with hydroxyapatite crystals, the presence of osteocalcin, and the absence of type 2 collagen, the predominant protein of cartilage, are also

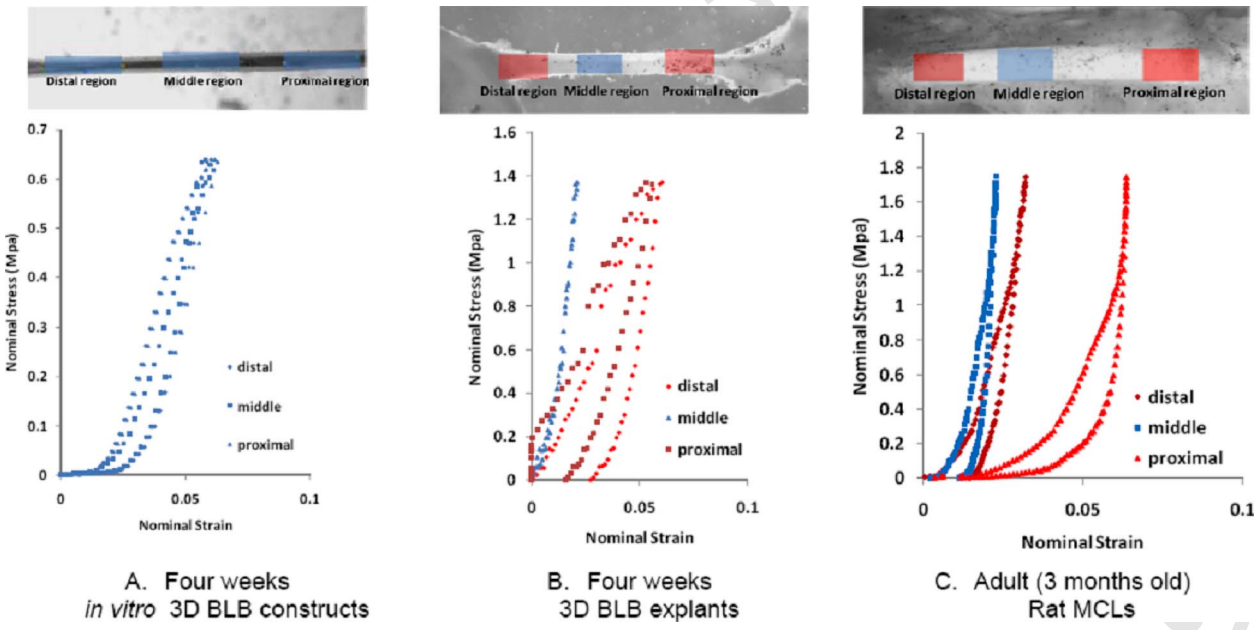

Fig. 10 Localized stress versus strain analysis of 3D BLB constructs in vitro (*a*), 3D BLB explants (*b*), and native rat MCL (*c*) with corresponding regions shown in the specimen photos. Developed for 4 weeks in vitro 3D BLB constructs show uniform strain response. After 1 month of implantation, strain responses are localized in 3D BLB explants, showing a functional gradient that is also indicated in native MCL. Regions that are closer to bones are relatively more compliant than the ligament midsections in both 3D BLB explants and native MCLs.

used as markers of a bone lineage and have been shown to be characteristics of in vitro EBC from BMSCs [13]. In addition, RUNX2 is used to visualize pre-osteoblasts in the periosteum, osteoblasts, and osteocytes in the bone, while CD31 is used to visualize the blood supply in the bone [28,29].

Ligament lineage from BMSC is characterized by type 1 collagen, the lack of mineralization, positive staining for elastin, and negative staining for collagen 2. The ligament portions of the 3D BLB constructs self-assemble in vitro around previously formed EBCs. The absence of DEX in the ligament media produces unmineralized ECM that displays evidence of the characteristic crimp morphology of type 1 collagen fibrils in vitro. The ligament region development in vivo includes increased collagen type 1 content, improved collagen organization and more consistent crimp morphology, and the development of a continuous aligned elastin network.

The incidence of ACL injury has been estimated at 1 in 3000 in the American population, with approximately 95,000 new injuries each year and combined with more than 50,000 knees that have such an injury are reconstructed annually [9]. These numbers are up to three- to fourfold from estimates of about a decade ago and are increasing rapidly in children. The preferred treatment for children with active growth plates is reconstruction using an allograft, but outcomes are limited by donor availability, biomechanical incompatibility, and immune rejection. The creation of an engineered ACL in vitro solely from BMSCs has the potential to greatly enhance outcomes in pediatric ACL reconstructions. Issues currently impeding clinical use of engineered tendons and ligaments include mechanical properties of the engineered graft that shield cells and inhibit neoligamentous tissue growth, challenges associated with integration between host bone and newly developed tissue and a rapid rate of scaffold degradation in vivo with a corresponding rate of tissue regeneration that is too slow [2]. The present approach avoids the use of a resorbable scaffold and adopts a design rubric based on the concept of displacement or strain controlled rather than load (or stress) controlled mechanical requirements of knee ligaments. Maximum strain levels during rehabilitation exercises in humans have been estimated at 0.05 (or 5%), which is approximately 25% of the failure strain in native knee ligament [9]. Our in vitro 3D BLB constructs are capable of withstanding repeated strain cycles in excess of 0.05. We tested the hypotheses that these constructs were capable of surviving the strain levels placed on the MCL of an adult rat during normal ambulatory motion and that the initial compliance of the ligament regions of the 3D BLB will allow cells within the construct to experience strains in vivo and deposit ligamentous ECM. None of the 3D BLB constructs failed in vivo. All implanted constructs were found to be well integrated to the native bone at the tibial and femoral insertions. After 1 month in vivo, the explanted BLB constructs showed physical growth from an average area of 0.17 ± 0.04 mm^2 in vitro to 0.25 ± 0.17 mm^2. Type 1 collagen was present throughout the cross section of the ligament portion of the 3D BLB explants. The changes in size and collagen constitution resulted in an increased geometrical stiffness P_{max}/length $=0.01$ N/mm in vitro versus P_{max}/length$=0.09$ N/mm in 3D BLB explants, as well as an increased tangent stiffness of 14.3 ± 3.0 MPa in vitro versus 34.6 ± 17.1 MPa in explants. The geometric stiffness of the 3D BLB explants significantly increased and has the same value compared with the stiffness of the 14 day native MCL (P_{max}/length$=0.09$ N/mm). The tangent stiffness of the 3D BLBs increased significantly from in vitro to explant values ($p=0.0309$) and the tangent stiffness of the 3D BLB explants did not differ significantly from that of the native MCLs (47.6 ± 22.9 MPa). None of the four 3D BLB explants failed during cyclic loading to approximately 10% strain indicating mechanically viable engineered interfaces (entheses). The average mechanical response is not sufficient to fully characterize the mechanical properties of ligament and tendon. Previous investigators demonstrated distinctly different strain behaviors along different portions of native MCL [30]. MCL flexion experiments by Arms et al. [31] demonstrated higher strain levels near bone insertions compared with the strain in the middle region where the joint line intersects. Investigations on biomechanical properties of tendon to bone enthesis by Thomopoulos et al. [32] also demonstrate an increased strain response near the tidemark in the entheses, where the unmineralized and mineralized fibrocartilage sections meet. Our present results for native adult MCL show a similar heterogeneous or functionally graded mechanical response that is consistent with these studies. The results from our implantation show that the engineered 3D BLB constructs adapted a functionally graded mechanical response in vivo that matches the heterogeneity of native MCL.

The purpose of the tube in the engineered construct implantations is to enable isolation of the constructs from the native tissue upon explantation primarily to facilitate mechanical testing. In previous studies, we have implanted our constructs without the silicone tube and they grew well but could not be extracted from the native tissue cleanly for mechanical tests. In our recent implantation studies without using tubing techniques, histology results from different sections of implanted engineered constructs actually show the portion outside of the tube advanced more rapidly in phenotype compared with the portion inside the tube. Possible explanations may be that the outer portions might have better access to the development of a vascularization system from the host animal. Further investigation developing several parallel studies is needed to gain more understanding.

The current design requirements of engineered tissue for ligament replacement aim to restore stability to the knee at the time of replacement. Many recent studies have shown that neither autogenous grafts nor scaffold-based engineered approaches ever attain the strengths of uninjured controls and that a large percentage (40–78%) of engineered ligaments have failed after a period of time in vivo [9,33]. We know of no previously published study in which the mechanical properties of an engineered ligament improved over time in vivo. We have speculated that the conditions required for rapid growth of normal collagen in ligament in vivo differ significantly from those required for collagen content maintenance. In particular, we targeted extensibility to withstand physiological strain levels and compliance to allow transduction of cellular signals, as two important design features of our engineered constructs. We further hypothesized that the ideal engineered ligament construct would exhibit nonlinear viscoelasticity, including strain rate dependence and hysteresis in cyclic loading, to more closely resemble the response of native tissue.

Histological characterization showed the differing characteristics of the bone and ligament parts of the 3D BLB constructs in vitro. Therefore, using our techniques, the BMSC has clearly gone to the proposed pathways and developed to ligament and bone as a result in vitro.

Foot print analysis showed no significant difference in rat motion function between presurgery and postimplantation surgery. As described in Sec. 3, the silicone tube surrounding the 3D BLB constructs was used to isolate the ligament portion from the surrounding soft tissue and as a marker for identification during explantation. During the surgery, the tube length was carefully adjusted so that only the freestanding portion of the ligament region was surrounded and therefore the tube was not in any way supporting or impeding the 3D BLB construct. The lack of a significant difference in foot print analysis indicates that the 3D BLB construct functioned well in the animal.

In conclusion, after either 1 or 2 months in vivo as a replacement for the MCL of a rat, the bone portion of 3D BLB constructs integrated well with the native bone. The ligament region of the rat 3D BLB constructs showed the presence of aligned, crimped, type 1 collagen, and elastin throughout, as well as an increased tangent modulus by a factor of 2.4. Following implantation, 3D BLB constructs grew in thickness and the cross-sectional area was on average twofold larger than that of the 14 day neonatal MCLs.

Load comparisons at the maximum cyclic strain levels of 10% during tensile testing reveal that the 3D BLB constructs were actually carrying higher loads without failure.

References

[1] Praemer, A., Furner, S., Rice, D. P., and Kelsey, J. L., 1992, *Musculoskeletal Conditions in the United States*, Am. Acad. Orthop. Surg., 1st ed.

[2] Goh, J. C.-H., Ouyang, H.-W., Teoh, S.-H., Chan, C. K. C., and Lee, E.-H., 2003, "Tissue-Engineering Approach to the Repair and Regeneration of Tendon and Ligaments," Tissue Eng., **9**, pp. 31–44.

[3] Linda, G. G., and Naughton, G., 2002, "Tissue Engineering: Current Challenges and Expanding Opportunities," Science, **295**, pp. 1009–1014.

[4] Petrigliano, F. A., McAllister, D. R., and Wu, B. M., 2006, "Tissue Engineering for Anterior Cruciate Ligament Reconstruction: A Review of Current Strategies," Arthroscopy: J. Relat. Surg., **22**(4), pp. 441–451.

[5] Freeman, J. W., Woods, M. D., and Larurencin, C. T., 2007, "Tissue Engineering of the Anterior Cruciate Ligament Using a Braid-Twist Scaffold Design," J. Biomech., **40**, pp. 2029–2036.

[6] Stoltz, J. F., Bensoussan, D., Decot, V., Netter, P., Ciree, A., and Gillet, P., 2006, "Cell and Tissue Engineering and Clinical Applications: An Overview," Biomed. Mater. Eng., **16**, pp. S3–S18.

[7] Van Eijk, F., Saris, D. B. F., Riesle, J., Willems, W. J., van Blitterswijk, C. A., Verbout, A. J., and Dhert, W. J. A., 2004, "Tissue Engineeirng of Ligaments: A Comparison of Bone Marrow Stromal Cells, Anterior Cruciate Ligament, and Skin Fibroblasts as Cell Source," Tissue Eng., **10**(5–6), pp. 893–903.

[8] Mascarenhas, R., and MacDonald, P. B., 2008, "Anterior Cruciate Ligament Reconstructions: A Look at Prosthetics—Past, Present and Possible Future," McGill J. Med., **11**(1), pp. 29–37.

[9] Frank, C. B., and Jackson, D. W., 1997, "The Science of Reconstruction of the Anterior Cruciate Ligament," J. Bone Jt. Surg., Am. Vol., **79**, pp. 1556–1576.

[10] Wang, I.-N. E., Shan, J., Choi, R., Oh, S., Kepler, C. K., Chen, F. H., and Lu, H. H., 2007, Role of Osteoblast-Fibroblast Interactions in the Formation of the Ligament-to-Bone Interface," J. Orthop. Res., **25**(12), pp. 1609–1620.

[11] Hairfield-Stein, M., England, C., Paek, H. J., Gilbraith, K. B., Dennis, R., Boland, E., and Kosnik, P., 2007, "Development of Self-Assembled, Tissue-Engineered Ligament From Bone Marrow Stromal Cells," Tissue Eng., **13**(4), pp. 703–710.

[12] Syed-Picard, F. N., 2006, "Development and Characterization of Three Dimensional, Scaffold-Less Bone and Ligament Tissues Engineered From Bone Marrow Stem Cells," , M.S. thesis, University of Michigan, Ann Arbor, MI.

[13] Syed-Picard, F. N., Larkin, L. M., Shaw, L. M., and Arruda, E. M., 2009, "Engineered Functional Bone From Bone Marrow Stromal Cells and Their Autogenous Extra-Cellular Matrix," Tissue Eng. Part A, **15**(1), pp. 187–195.

[14] Larkin, L. M., van der Meulen, J. H., Dennis, R. G., and Kennedy, J. B., 2006, "Functional Evaluation of Nerve-Skeletal Muscle Constructs Engineered In Vitro," In Vitro Cell. Dev. Biol., **42**, pp. 75–82.

[15] Larkin, L. M., Calve, S., Kostrominova, T. Y., and Arruda, E. M., 2006, "Structural and Functional Evaluation of Tendon-Skeletal Muscle Constructs Engineered In Vitro," Tissue Eng., **12**, pp. 3149–3158.

[16] Urbanchek, M. S., Chung, K. C., Asato, H., Washington, L. N., and Kuzon, W. M., 1999, "Rat Walking Tracks Do Not Reflect Maximal Muscle Force Capacity," J. Reconstr Microsurg, **15**, pp. 143–149.

[17] Alhadlaq, A., and Mao, J. J., 2004, "Mesenchymal Stem Cells: Isolation and Therapeutics," Stem Cells Dev., **13**, pp. 436–448.

[18] Maniatopoulos, C., Sodek, J., and Melcher, A. H., 1988, "Bone Formation In Vitro by Stromal Cells Obtained From Bone Marrow of Young Adult Rats," Cell Tissue Res., **254**, pp. 317–330.

[19] Deepica, R., McCarthy, M., and Gronowicz, G. A., 1997, "Ascorbic Acid Alters Collagen Integrins in Bone Culture," Endocrinology, **138**, pp. 3606–3612.

[20] Scutt, A., and Bertram, P., 1999, "Basic Fibroblast Growth Factor in the Presence of Dexamethasone Stimulates Colony Formation, Expansion, and Osteoblastic Differentiation by Rat Bone Marrow Stromal Cells," Calcif. Tissue Int., **64**, pp. 69–77.

[21] Noff, D., Pitaru, S., and Savion, N., 1989, "Basic Fibroblast Growth Factor Enhances the Capacity of Bone Marrow Cells to Form Bone-Like Nodules In Vitro," FEBS Lett., **250**, pp. 619–621.

[22] Pitaru, S., Kotov-Emeth, S., Noff, D., Kaffuler, S., and Savion, N., 1993, "Effect of Basic Fibroblast Growth Factor on the Growth and Differentiation of Adult Stromal Bone Marrow Cells: Enhanced Development of Mineralized Bone-Like Tissue in Culture," J. Bone Miner. Res., **8**, pp. 919–929.

[23] Locklin, R. M., Oreffo, R. O. C., and Triffitt, J. T., 1999, "Effects of TGFbeta and bFGF on the Differentiation of Human Bone Marrow Stromal Fibroblasts," Cell Biol. Int., **23**, pp. 185–194.

[24] Ronchetti, I. P., Quaglino, D., Jr., and Bergamini, G., 1996, *Ascorbic Acid and Connective Tissue, Subcellular Biochemistry, Volume 25: Ascorbic Acid: Biochemistry and Biomedical Cell Biology*, Plenum, New York, p. 249.

[25] Martin, I., Shastri, V. P., Padera, R. F., Yang, J., Mackay, A. J., Langer, R., Vunjak-Novakovic, G., and Freed, L. E., 2001, "Selective Differentiation of Mammalian Bone Marrow Stromal Cells Cultured on Three-Dimensional Polymer Forms," J. Biomed. Mater. Res., **55**, pp. 229–235.

[26] Marui, T., Niyibizi, C., Georgescuhi, C. M., Kavalkovich, K. W., Levine, R. E., and Woo, S. L.-Y., 1997, "Effect of Growth Factors on Matrix Synthesis by Ligament Fibroblasts," J. Orthop. Res., **15**, pp. 18–23.

[27] Nauman, E. A., Sakata, T., Keaveny, T. M., Halloran, B. P., and Bikle, D. D., 2003, "bFGF Administration Lowers the Phosphate Threshold for Mineralization in Bone Marrow Stromal Cells," Calcif. Tissue Int., **73**, pp. 147–152.

[28] Marie, P. J., 2008, "Transcription Factors Controlling Osteoblastogenesis," Arch. Biochem. Biophys., **473**, pp. 98–105.

[29] Woodfin, A., Voisin, M.-B., and Noirshagh, S., 2007, "PECAM-1: A Multi-Functional Molecule in Inflammation and Vascular Biology," Arterioscler. Thromb. Vasc. Biol., **27**, p. 2514.

[30] Warren, L. F., Marshall, J., and Girgus, F., 1974, "The Prime Static Stabilizer of the Medial Side of the Knee," J. Bone Jt. Surg., Am. Vol., **56-A**, pp. 665–674.

[31] Arms, S., Boyle, J., Johnson, R., and Pope, M., 1983, "Strain Measurement in the Medial Collateral Ligament of the Human Knee: An Autopsy Study," J. Biomech., **16**(7), pp. 491–496.

[32] Thomopoulos, S., Marquez, J. P., Weinberger, B., Birman, V., and Genin, G. M., 2006, "Collagen Fiber Orientation at the Tendon to Bone Insertion and Its Influence on Stress Concentrations," J. Biomech., **39**, pp. 1842–1851.

[33] Heimstra, L. A., Webber, S., MacDonald, P. B., and Kriellaars, D. J., 2007, "Contralateral Limb Strength Deficits After Anterior Cruciate Ligament Reconstruction Using a Hamstring Tendon Graft," Clin. Biomech. (Bristol, Avon), **22**, pp. 543–550.

PROOF COPY [BIO-08-1389] 043910JBY